Research Article

The use of GIS and water quality index to assess groundwater quality of krimat aquifer (Essaouira; Morocco)

Otman El Mountassir[1] · Mohammed Bahir[1,2] · Driss Ouazar[2] · Salah Ouhamdouch[1] · Abdelghani Chehbouni[2,3] · Mohamed Ouarani[2]

Abstract
The aim of this present study was to evaluate groundwater quality in the upstream part of the Essaouira basin. A detailed geochemical study of groundwater region is described, and the origin of the chemical composition of groundwater has been qualitatively evaluated, using multivariate statistical methods (PCA, HCA), and Water Quality Index (WQI) was used to determine the suitability of water for drinking. To attempt this investigation, 38 samples were analysed for various physicochemical parameters such as temperature, pH, TDS, Na, NO_3, K, Ca, HCO_3, Cl, Mg, and SO_4. The results obtained showed that the facies characterizing the study area was a combination of Ca–SO_4 and mixed Ca–Mg–Cl. Hydrochemical approach based on the bivariate diagrams of major ions indicates that the origins of groundwater mineralization are the result of (I) evaporite dissolution; (II) cation-exchange reactions; and (III) evaporation processes. The WQI values range from 82.3 to 390.9, and therefore the water samples can be categorized into five groups: excellent water to water unsuitable for drinking. In global, 61% of the groundwater sampled had poor water quality, 18% were very poor water quality, 16% are unsuitable for drinking, and just 6% represent a good quality. However, the results of this paper indicate that most water is not safe for drinking and needs further treatment.

1 Introduction

Water is a fundamental human need and according to the statistics groundwater is the main source of drinking water for more than 1.5 billion people in the world[1]. With a better understanding of the importance of drinking water quality to human health, there is a great need to assess groundwater quality [2]. Moreover, it is a need for studies on how groundwater will be managed. For efficiency, the management and assessment of groundwater resources need an understanding of hydrogeochemical and hydrogeological features of the aquifer [3, 4]. Furthermore, groundwater quality depends on several components such as topographic relief, rainfall, mineral dissolution, ion exchange, oxidation, reduction, human and natural activities, use of fertilizers and pesticides [5–8].

In arid and semi-arid areas, principally in coastal areas, an increase in the salinity is being confirmed in most of the major aquifers being used for water supply in coastal regions, which led to the deterioration in water quality [9–14]. This deterioration is due to the inflow of saline water because of over-exploitation of groundwater, and/or mobilization of saline formation waters (combining with ancient seawater trapped in the sediments). However, the assessment of groundwater quality in these areas is essential for better management and protection of this resource.

✉ Otman El Mountassir, otman.elmountassir@ced.uca.ma | [1]High Energy and Astrophysics Laboratory, Faculty of Sciences Semlalia, Cadi Ayyad University, Marrakech, Morocco. [2]IWRI Mohammed VI Polytechnic University, Hay My Rachid, 43150 Ben Guerir, Morocco. [3]CESBIO, Université de Toulouse, CNRS, CNES, IRD, BPI 280, 31065 Toulouse CEDEX 9, France.

In recent decades, several tools have been used to quantify status and water chemistry. Among these tools, the water quality index [15, 16] is one of the most effective tools for assessing and obtaining a comprehensive picture of groundwater quality. It is a mathematical technique used to transform high quantities of water characterization data into one simple indicator that expresses overall water quality, to differentiate between very clean water and polluted water at some location and time [17–21].

Essaouira Basin, the subject of this study, is one of the semi-arid basins of Morocco. In this coastal basin, groundwater is the main water resource. During the last decades, this basin has experienced a succession of drought episodes under the climate change effect leading to a qualitative and quantitative degradation of this resource [22].

However, the main objective of this study is to evaluate and map the groundwater quality status of krimat aquifer situated in Northwestern Morocco by using Water Quality Index and Geographic Information System.

2 Study area

The Ouazi Basin is located in the east and north of the Essaouira city between the coordinates 100,000 and 140,000 (m) for the X and between 80,000 and 140,000 (m), 31°23′53.12″N and 9°25′45.78″W (geographic system projection), with an area of 1000 km^2 (Fig. 1). It is limited in the north by Hadid anticline, by Meskala region in the south, by Mramer wadi in the east, and Atlantic Ocean in the west. This basin is controlled by a semi-arid climate, with an average annual rainfall of 300 mm and temperatures of 20 °C [23]. In geomorphological terms, the Essaouira synclinal zone is less rugged, with a lower relief characterized by low hills and shaped by a sparse water system. Concerning the hydrogeological aspect, the Ouazzi Wadi sub-basin is a sedimentary basin, mainly composed of two main aquifers (Fig. 1). The first is the Plio-Quaternary phreatic aquifer with marine or dune sandstone–limestone matrix, and a primary hydraulic conductivity due to porosity. The wall of this aquifer is formed by the Senonian grey marls; the subcrop anti-Pliocene shows that the Plio-Quaternary can be in direct contact with the Triassic and Cretaceous other levels [24]. The second is the Cenomanian–Turonian carbonate aquifer; it is mainly formed by limestones and dolomitic-limestone layers (Fig. 1). The base of the Cenomanian–Turonian system corresponds to lower Cenomanian grey clays and the top to the Senonian white marls [25]. This reservoir is the main food resource of drinking water of Essaouira city as well as the surrounding villages. It is also a source of modest agricultural use (food-type) [26]. In addition, the chemical composition of groundwater is controlled by many factors that include composition of precipitation, geological structure, and mineralogy of the watershed sand aquifers and geochemical processes within the aquifer [27–30]. The piezometric study shows that the natural discharge zone of the studied aquifer is the Atlantic Ocean and that the groundwater flows mainly from south-east to north-west upstream and from east to west downstream (Fig. 1). This direction of flow is conditioned by the geometry of the aquifer and the tectonic.

3 Materials and methods

3.1 Chemical analysis

Groundwater samples were collected in March 2018, from 38 wells capturing the krimat aquifer and representing a homogeneous spatial distribution on the whole aquifer (Fig. 1).

A portable GPS was used to locate the sampling wells and polyethylene bottles were carefully rinsed two to three times by the water collected before filling. The physicochemical parameters (pH, temperature, electrical conductivity) were measured in situ immediately after sample collection, using the Multi-parameter HI 9828. The depth of the water level was measured using a piezometric probe with 200 m of length.

Chloride ions are determined by Mohr's method. Concentrations of HCO_3 were determined by titration, using 0.1 N HCl. Sodium (Na) and potassium (k) ions are determined by flame atomic absorption spectrometry. The sulphates are determined by spectrophotometry method using a Hach Lange DR 3800 spectrophotometer. Concentrations of calcium by following the complexometry (EDTA) and magnesium (Mg) were obtained from total hardness. These chemical analyses were carried out at the Laboratory of Geosciences and Environment (LGE) of Ecole Normale Superieure, of Marrakech, Morocco. The accuracy of the chemical analysis was verified by calculating ion balance errors in Eq. (1), which is based on the principle that the sum of major anions and the sum of the major cations are equivalent (concentrations expressed as (meq/L)) and the error in % is given by (1)

$$IB = \left(\frac{\sum_{\text{cations}} - \sum_{\text{anions}}}{\sum_{\text{cations}} + \sum_{\text{anions}}} \right) \times 100 \qquad (1)$$

A chemical analysis of the waters is not considered representative and acceptable only when the ionic balance is equal to or less than 10% [31].
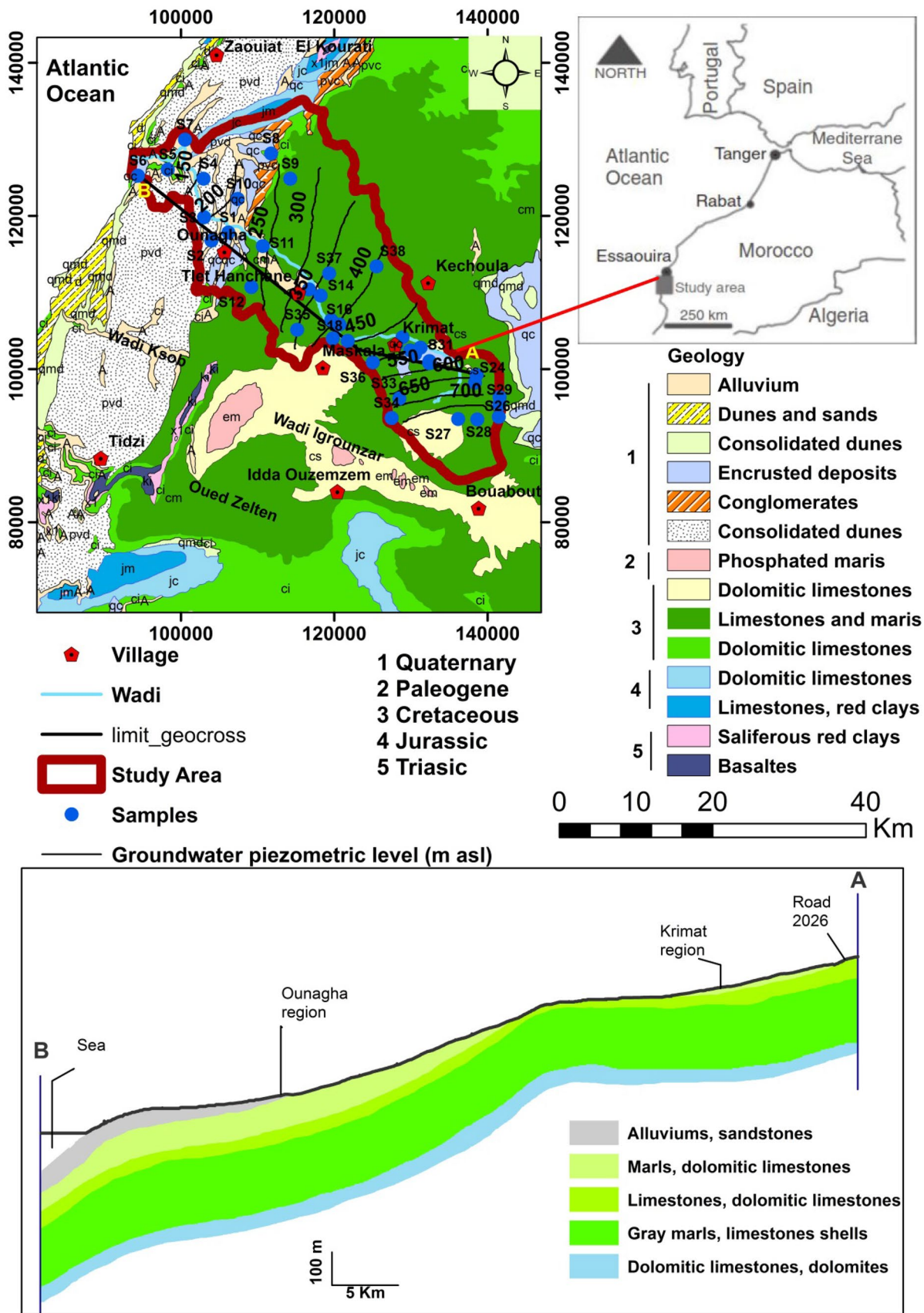
Fig. 1 Geographic situation, location of groundwater sampled points in Wadi Ouazi basin, geological and cross section of the study area

3.2 GIS analysis

There are two main interpolation techniques: deterministic and geostatistics. Deterministic interpolation techniques create a surface from measured points, based on their extent of similarity [e.g. inverse distance weighted (IDW)] or the degree of smoothing (e.g. radial basis functions). Geostatistical interpolation techniques utilize the statistical properties of the measured points [32].

For this study, a weighted inverse distance interpolation (IDW) method was used to produce thematic spatial distributions for each parameter: EC, TDS, pH, NO_3, Ca, Mg, K, Na, Cl, HCO_3 and SO_4, and water quality index (WQI) of the study area of krimat aquifer. Interpolation technique is the procedure of predicting unknown values using the known values in the vicinity. This technique uses a defined or selected area of sample points to estimate the value of the output grid cell.

3.3 Water quality index

The WQI is a very simple technique for evaluating the overall water quality of any region and communicating this information with the decision-makers; analysis of the water samples for various parameters is done as per WHO standards [33]. From the estimation of a water quality index is determined the degree of pollution of groundwater by using Geographical Information System Software (GIS) issues by integrating complex data and generating a score, which ultimately describes the water quality status [34–36]. The methodology used is summarized in the flowchart established in Fig. 2. The results of the physicochemical analyses are summarized in (Table 1).

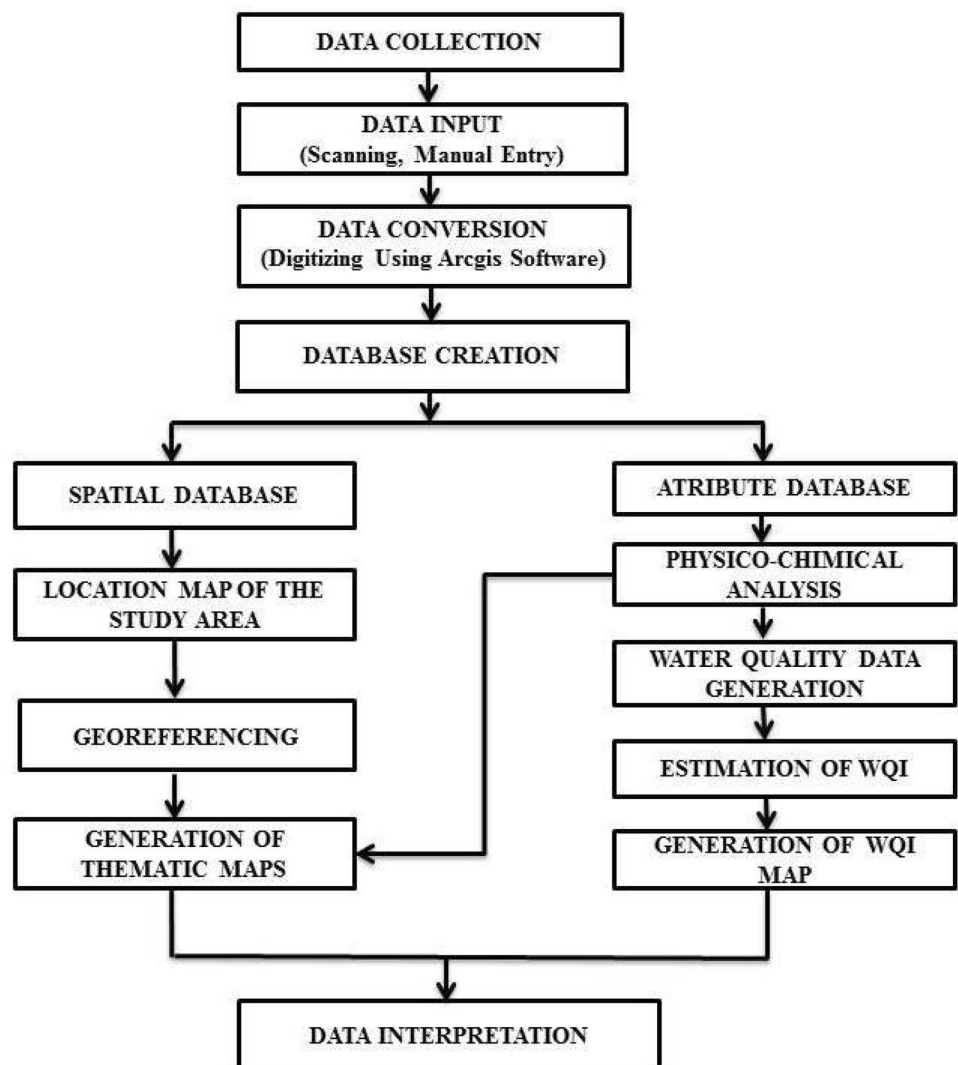**Fig. 2** Flow-chart of the methodology adopted

Table 1 Physicochemical parameters of groundwater samples of study areas

No	T	pH	EC	TH	TDS	Cl	SO$_4$	NO$_3$	HCO$_3$	Na	Ca	Mg	K
	°C		µs/cm	mg/l									
S1	22.6	7.53	1925	703.3	958	369.2	178.5	48.6	433.2	119.8	133.1	90.4	4.9
S2	23.4	7.24	2769	1126.5	1387	582.2	291.6	37.0	482.0	176.0	189.2	159.4	3.0
S3	22.3	7.25	2793	918.9	1400	624.8	284.3	40.0	396.6	176.0	158.7	127.3	2.1
S4	22.4	7.15	3363	1102.8	1686	781.0	294.1	33.8	433.2	232.2	200.4	146.8	3.6
S5	21.2	7.65	2216	647.2	1117	482.8	161.3	20.0	414.9	187.9	113.8	88.5	0.3
S6	20.4	7.33	4062	887.9	2031	908.8	163.8	165.6	335.6	300.3	221.2	81.6	20.9
S7	20.8	7.67	1650	383.9	825	383.4	67.9	13.0	360.0	180.7	93.0	36.9	0.8
S8	21.8	7.35	2198	775.2	1095	511.2	48.2	7.2	634.6	158.3	144.3	101.1	7.5
S9	21.7	7.25	2152	615.3	1077	468.6	65.4	31.1	512.5	182.0	112.2	81.6	3.0
S10	21.6	7.34	3184	1055.6	1597	766.8	213.0	76.4	274.6	208.6	248.5	105.9	25.9
S11	23.0	7.47	2200	775.0	1101	468.6	185.9	27.0	427.1	140.5	133.1	107.9	2.7
S12	21.6	7.56	4372	1349.6	2188	1164.4	210.5	60.5	433.2	303.3	184.4	216.8	2.4
S13	21.9	7.88	2141	1046.6	1070	284.0	363.0	64.5	427.1	99.1	174.7	148.7	6.3
S14	22.4	8.36	2359	983.0	1180	355.0	215.4	7.0	689.5	105.0	186.0	126.4	11.7
S15	21.7	7.47	2170	1030.3	1082	312.4	313.8	24.3	604.1	128.7	152.3	158.4	4.1
S16	22.9	7.8	2214	894.9	1106	397.6	328.5	6.0	457.6	128.7	158.7	121.5	2.9
S17	23.1	7.23	3256	2183.2	1631	184.6	1361.3	3.5	372.2	57.7	513.0	219.7	4.3
S18	20.6	7.65	2429	815.0	1216	497.0	139.2	18.0	402.7	275.6	139.5	113.7	2.2
S19	20.4	7.32	4802	2156.6	2404	823.6	751.5	166.0	500.3	264.8	322.2	329.5	2.8
S20	17.9	7.85	2196	991.2	1099	284.0	372.8	60.6	262.4	95.7	200.4	119.6	5.3
S21	18.5	7.65	2801	1230.9	1401	440.2	458.9	35.5	347.8	155.3	240.5	153.6	7.3
S22	22.0	7.34	1248	499.8	626	184.6	11.3	21.6	335.6	37.0	117.0	50.5	1.8
S23	16.2	8.14	1350	671.5	674	170.4	119.5	18.2	329.5	34.0	141.1	77.8	2.5
S24	17.0	7.65	3691	2375.5	1848	241.4	2221.2	8.0	311.2	75.4	583.6	223.6	1.9
S25	20.7	7.47	1966	975.1	981	355.0	335.9	17.2	378.3	57.7	187.6	123.4	6.0
S26	16.2	7.91	1747	559.7	874	198.8	88.3	82.7	286.8	96.2	125.0	60.3	6.8
S27	18.5	7.83	1297	447.6	649	227.2	85.5	33.5	360.0	81.4	85.0	57.3	4.8
S28	20.5	7.67	1624	783.3	813	213.0	343.3	7.0	335.6	87.3	153.9	97.2	4.5
S29	19.9	7.52	1571	806.9	786	213.0	289.2	33.2	353.9	96.2	134.7	114.7	2.4
S30	23.2	7.57	1163	679.2	581	198.8	176.1	19.3	329.5	37.0	123.4	90.4	2.3
S31	18.4	7.76	1198	503.9	599	213.0	65.4	19.0	317.3	63.6	121.8	48.6	3.8
S32	21.5	7.55	1694	735.5	847	255.6	220.3	35.1	347.8	63.6	157.1	83.6	2.7
S33	20.4	7.93	809	399.5	404	99.4	45.7	15.6	372.2	10.4	72.1	53.5	0.8
S34	20.4	7.76	778	375.5	390	142.0	43.3	19.0	299.0	19.2	65.7	51.5	0.6
S35	19.7	8.15	4133	2413.1	2069	681.6	1184.3	6.4	488.1	182.0	426.5	328.5	5.5
S36	19.3	8.75	1386	671.3	694	213.0	227.7	12.2	347.8	60.7	125.0	87.5	6.6
S37	21.0	8.49	1600	439.9	800	369.2	58.0	28.3	256.3	143.5	105.8	42.8	0.4
S38	19.5	8.83	5041	1789.8	2520	1178.6	633.4	23.0	396.6	279.6	312.6	245.9	36.5
Min	16.2	7.15	778	375.5	390	99.4	11.3	3.5	256.3	10.4	65.7	36.9	0.3
Max	23.4	8.83	5041	2413.1	2520	1178.6	2221.2	166	689.5	303.3	583.6	329.5	36.5
Mean	20.7	7.7	2356.5	968.4	1179.1	427.5	332.0	35.4	396.0	134.2	185.7	123.0	5.6
SD	1.9	0.4	1087.2	541.8	544.4	271.3	424.9	36.8	98.1	81.1	112.5	71.5	7.2

4 Results and discussion

4.1 Groundwater hydrochemical facies

Hydrochemical facies is a useful tool for determining groundwater chemistry. It is used to represent the similarity and dissimilarity in the chemistry of groundwater samples based on the anions and dominant cations of all samples [37, 38]. In addition, these trilinear diagrams used for tracing hydrochemical data were independently developed by [39, 40].

The projection of the analysed samples on the Piper diagram (Fig. 3) shows that the majority of the samples are Ca–Mg–Cl, while two points have a Ca–SO$_4$ facies.

In order to highlight the different mechanisms that contribute to groundwater mineralization, the relationships between major elements were investigated in several bivariate diagrams plotted (Fig. 4). These diagrams that were plotted take into account the most abundant minerals (calcite, dolomite) and evaporates (halite, gypsum) generally existing in sedimentary deposits.

The binary diagram for Na and Cl (Fig. 4a) shows a positive correlation between these two ions, with $R^2 = 0.83$ for the Ouazzi basin. This positive correlation indicates the same source of the two ions. Some samples are close to the halite dissolution line. Other samples are placed below the line, indicating a deficit of Na v Cl; this Na deficit is balanced by an excess of Ca^{2+} and Mg^{2+}, indicating a cation-exchange process [14].

The correlation diagram for Ca and Mg (Fig. 4b) shows a positive correlation between the two cations reflecting the same source with $R^2 = 0.60$. A few samples are plotted around the dissolution line of dolomite, indicating a limited contribution of this mineral to groundwater mineralization [9].

The correlation between Ca and SO$_4$ (Fig. 4c) shows a high positive correlation between these two ions in the samples with $R^2 = 0.89$. This positive correlation indicates that these two ions have the same source. In addition, Fig. 4c shows that only few samples are close to the dissolution line of gypsum, indicating that the dissolution of gypsum and anhydrite is limited [25].

The relationship between Ca and HCO$_3$ (Fig. 4d) is low with $R^2 = 0.013$. This weak correlation supports the absence of a relationship between these two ions. From Fig. 4d, it can be seen that the Ca$_2$ concentration increases, while the HCO$_3$ concentration remains relatively constant [9].

4.2 Multivariate statistical analysis

To understand different water types in the study area, statistical approach of the obtained results must be of high importance. However, hierarchical clustering analysis method (HCA) and principal component analysis (PCA) are used to distinguish between water groups that have similarities in hydrochemical composition [41]. Indeed, HCA and PCA were carried out on 38 individuals (water samples) and 9 variables (TDS and 8 major elements) using Ward method with Euclidean distance.
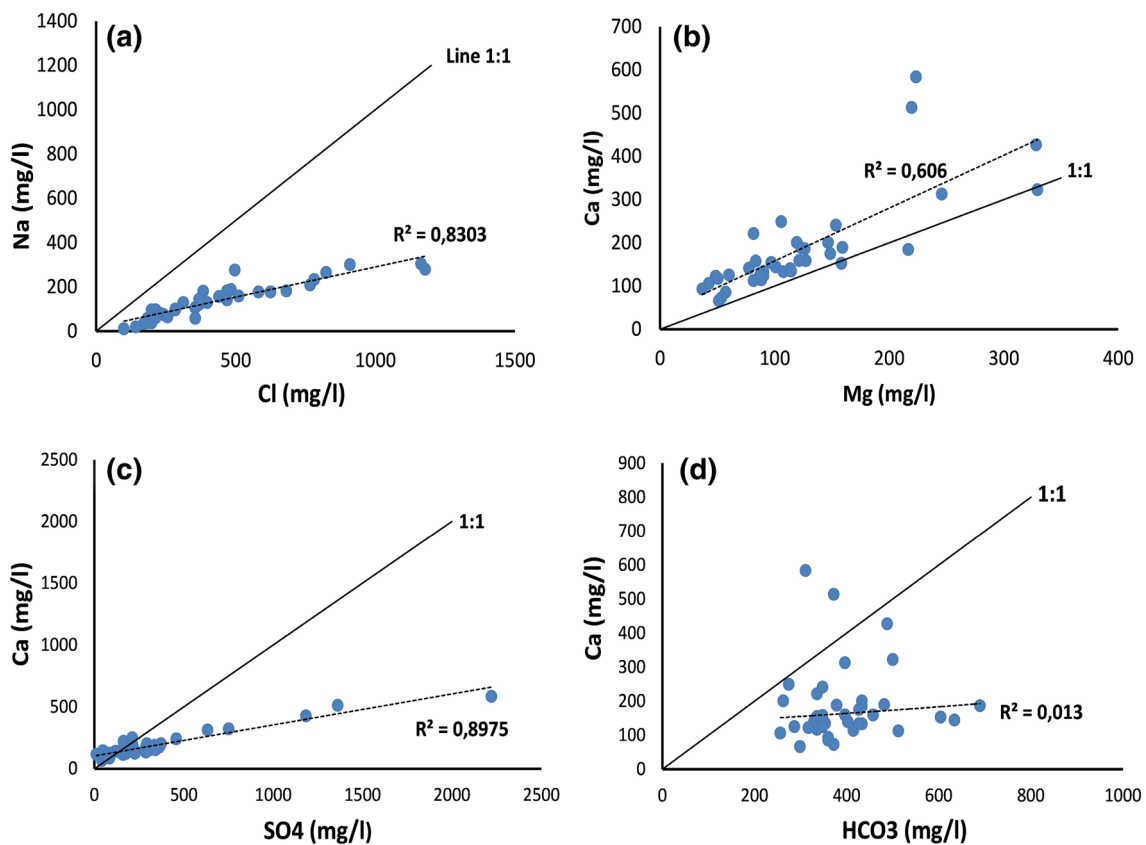
Fig. 3 Piper trilinear diagram
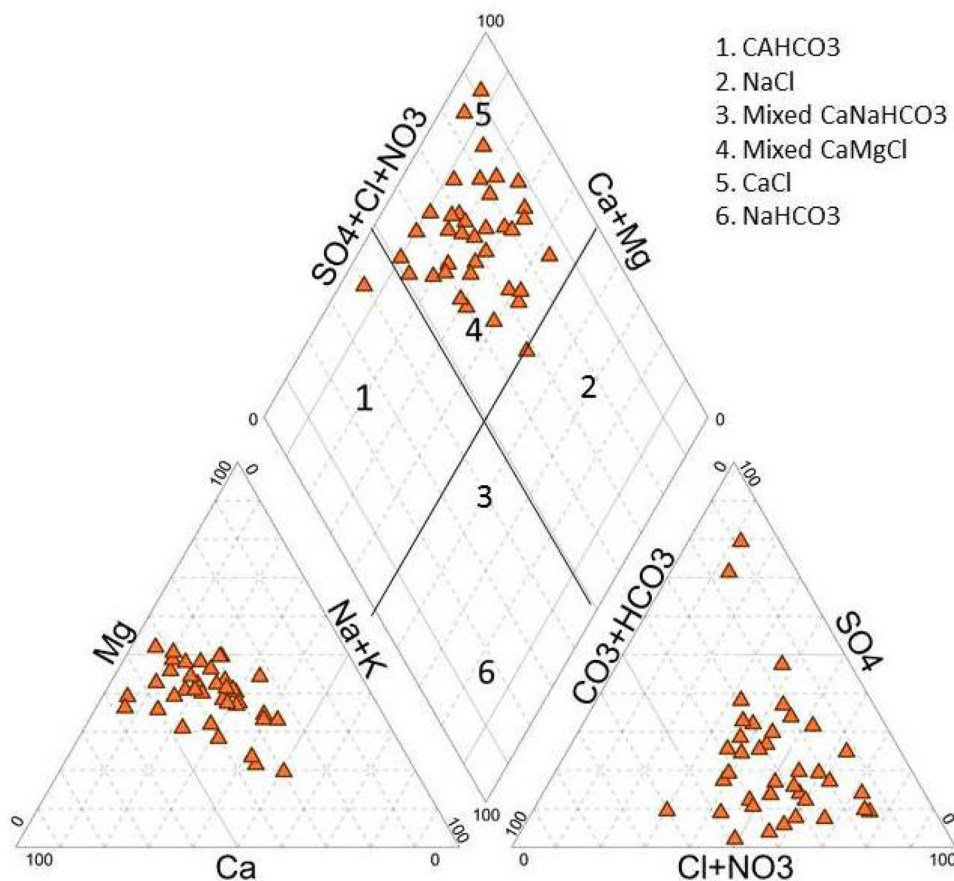
Fig. 4 Correlation diagram: **a** Na versus Cl; **b** Ca versus Mg; **c** Ca versus SO_4; **d** Ca versus HCO_3

Dendrogram of variables allowed separating two groups (Fig. 5). Group 1 is formed by SO_4, Cl, and HCO_3, while group 2 is formed by Ca, Mg, NO_3, Na, and K. The correlation between these variables is presented in Table 2.

As shown in Table 2, TDS, Na, and Cl have a strong correlation with a correlation coefficient of 0.77 and 0.85, respectively. This suggests that the dissolution of evaporitic minerals and the paleo-seawater intrusion contribute to the groundwater mineralization in the study area [2, 42]. The strong positive correlation between Ca and Mg indicates that they are probably due to carbonate and dolomite dissolution, base exchange, and paleo-seawater intrusion [2, 42]. The low correlation between HCO_3 and Ca (0.03) and between HCO_3 and Mg (0.35) confirms the contribution of carbonate mineral dissolution and paleo-seawater intrusion in the groundwater mineralization in the study area. A strong positive correlation between SO_4 and Ca was observed. This correlation is probably due to the evaporitic mineral dissolution. The weak correlation between SO_4 and NO_3 with a correlation coefficient of − 0.08 confirms this hypothesis.

Variable projection on the F1–F2 plane, which explains 71.12% of the total variance, indicates that all the variables, except NO_3 and HCO_3, are positively correlated

with the F1 axis (Fig. 3). As a result, this axis represents the cluster responsible for the mineralization of water in the study area. However, the more the F1 axis components are positive, the more the wells have a high concentration of major ions (Fig. 6). NO_3 and HCO_3 are positively correlated with the F2 axis; therefore, the positive components on this axis are enriched by the nitrates and the bicarbonate. This reflects the presence of another phenomenon responsible for these ions [14].

4.3 Physicochemical parameters

Groundwater temperatures (Table 1) varied from 16.2 to 23.4 °C, with an average and standard deviation values of 20.7 °C, and 1.9 °C, respectively.

The pH values vary from 7.15 to 8.83 (Table. 1) indicating that groundwater is slightly alkaline. All samples had a pH values within the acceptable limit "6.5–8.5" except two samples with values above the permissible limit fixed by WHO [33]. Usually, pH has no direct impact on consumers. It is one of the most important operational water quality parameters with the optimum pH required often being in the range of 7.0–8.5 by WHO [33]. The spatial distributions of pH concentrations (Fig. 7) shown that the majority of
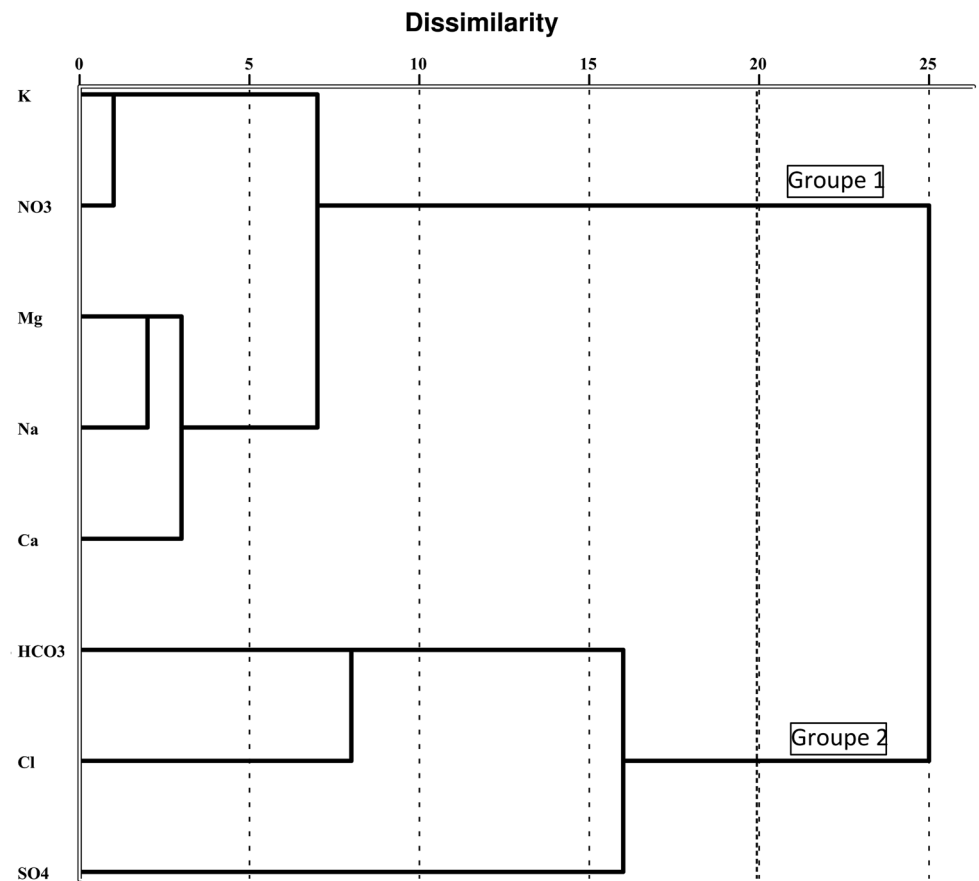
Fig. 5 Dendrogram of variables

Dissimilarity

Table 2 Correlation matrix of the major ions and the TDS for the study area

	TDS	Ca	Mg	Na	K	Cl	HCO$_3$	SO$_4$	NO$_3$
TDS	1								
Ca	0.70	1							
Mg	0.83	0.78	1						
Na	0.77	0.17	0.43	1					
K	0.50	0.25	0.21	0.41	1				
Cl	0.85	0.26	0.54	0.91	0.55	1			
HCO3	0.25	0.03	0.35	0.27	0.00	0.25	1		
SO4	0.54	0.95	0.71	0.01	0.05	0.07	−0.01	1	
NO3	0.44	0.06	0.19	0.48	0.28	0.44	−0.10	−0.08	1

the samples have a neutral pH with value below the desirable limit.

As for conductivity, it informs on the quantity of ionic matter dissolved in water and depends on the nature of the soil. According to WHO [33], the desirable limit of EC for drinking water is fixed at 1500 µs/cm. For the analysed samples, the EC varies between 578 and 5041 µs/cm with an average of 2356 µs/cm. The spatial distribution of EC (Fig. 7) shows that more than 90% of water samples are not permissible for drinking.

As for TDS, the low values (390–874 mg/l) were observed in samples S1, S3-9, S15, S18, and S23 (Fig. 7),

while the rest of the samples show high values (958 to 2520 mg/l), from east to west direction of groundwater flow. According to WHO standards, 70% of samples exceed the permitted limits. However, the majority of the wells tested are unsuitable for direct consumption without prior treatment.

Chlorides are inorganic anions contained in varying concentrations in natural waters. In the study area, the chloride (Cl) concentrations range from 99.4 to 1178.6 mg/l with an average of 427.5 mg/l (Table. 1, Fig. 8). The standard values prescribed by the WHO for chloride concentration are 250 mg/l. It was found that chloride concentration
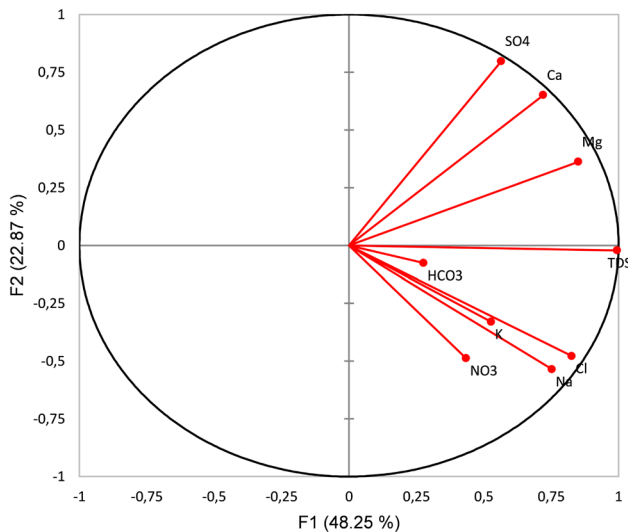
Fig. 6 Principal component analyses; variables projection on F1 and F2 plane

of all samples of exceeds the maximum allowable limit. These high levels of Cl are mainly due to the dissolution of halite [10]. The sodium concentration in the study varies between 10.4 and 303.3 mg/l with an average value of 134.2 mg/l (Table. 1, Fig. 8).

Calcium and magnesium in water are used to assess the appropriateness of water use. In addition, Ca and Mg are directly related to the hardness of the water. This increases with the increase in magnesium and calcium levels. For the study area, calcium concentrations range from 65.7 to 583.6 mg/l, with an average value of 185.7 mg/l (Table. 1, Fig. 8). As for the magnesium, it varies between 36.9 and 329.5 mg/l with an average value of 123 mg/l (Table. 1, Fig. 8).

Sulphates are found in natural waters as SO_4 ions with very different concentrations. According to the WHO [33], the concentration of sulphate (SO_4) in water can probably react with human organs if it exceeds the maximum allowed limit of 400 mg/l and causes a laxative effect on the human system with the excess of magnesium. For the analysed samples, the sulphate contents vary between 11.3 and 2221.2 mg/l and the average concentration of the sulphate index is 332 mg/l. However, the waters of the study area are below the recommended limit. The spatial distribution of the groundwater sulphate concentration in the study area (Fig. 8) shows that only S17, S19, S24, S35, and S38 show concentrations above 600 mg/l, reflecting poor quality (not permissible).

The concentration of bicarbonates (HCO_3) in natural waters depends on carbon dioxide, pH, cations, temperature, and more dissolved salts. For the study zone, the bicarbonate concentrations vary between 256.3

and 689.5 mg/l with an average of 396 mg/l. All samples exceeding the permissible limits of bicarbonate (200 mg/l) thus reflect a poor quality of the groundwater with respect to this ion.

Potassium is generally the least abundant element in water after Na, Ca, and Mg. It contributes very little to the mineralization of natural water. In the study area, the potassium concentration ranges from 0.3 to 36.5 mg/l (Fig. 8) with an average value of 5.6 mg/l. All samples had a potassium value within acceptable limits with the exception of three samples S6, S10, and S38 with values above the allowable limit (12 mg/l).

As for nitrate contents, they range from 3.5 to 166 mg/l with a mean value equal to 35.4 mg/l (Table. 1). Some samples exceed the permissible limit of 45 mg/l (WHO). High concentrations of NO3 would come from domestic pollutants. Only the catchment points are polluted and this pollution originates from the traditional methods of drawing. These result in a significant amount of water flowing around the catchment wells, constituting quasi-permanent pools that are enriched in NO3 by livestock waste during watering [43].

5 WQI

5.1 Estimation of water quality index (WQI)

The WQI has been calculated to evaluate the suitability of groundwater quality for drinking purposes of the krimat aquifer. The selection of the parameters that will make up the index depends on several factors, such as the purpose of the index, the importance of the parameter, and the availability of data. Physicochemical parameters TDS, pH, EC, Cl, SO_4, HCO_3, NO_3, Ca, Mg, Na, and K were determined.

Four steps are followed to estimate WQI. In the first step, we have chosen onz parameters and each of the parameter has been assigned a weight (wi) conforming to the relative importance in the overall water quality (Table. 3).

The top weight 5 was assigned to nitrate (NO_3) and total dissolved solids (TDS), considering that these often influence groundwater quality the most, weight 4 has been assigned to pH, electrical conductivity (EC), and sulphate (SO_4), weight 3 has been assigned to chloride (Cl) and bicarbonate (HCO_3), and weight 2 has been assigned to parameters potassium (K), calcium (Ca), and sodium (Na) depending on their signification in the overall quality of water for drinking purposes. The minimum weight 1 has been assigned to parameter magnesium (Mg) which rarely plays an insignificant role in groundwater quality.

In the second step, the relative weight (Wi) is computed by Eq. (2) using a weighted arithmetic index method given below [15, 16] and the following steps [44–47].
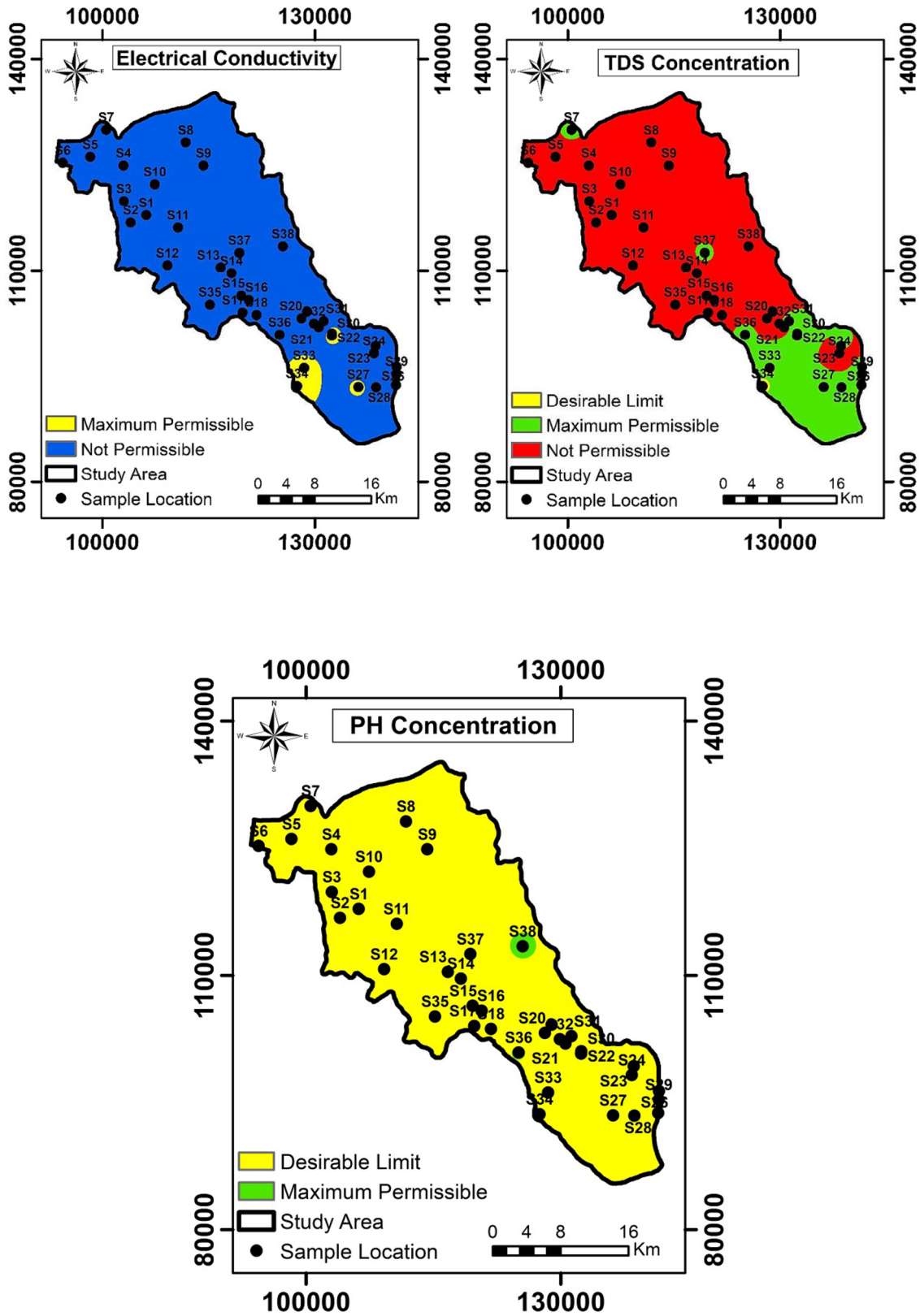
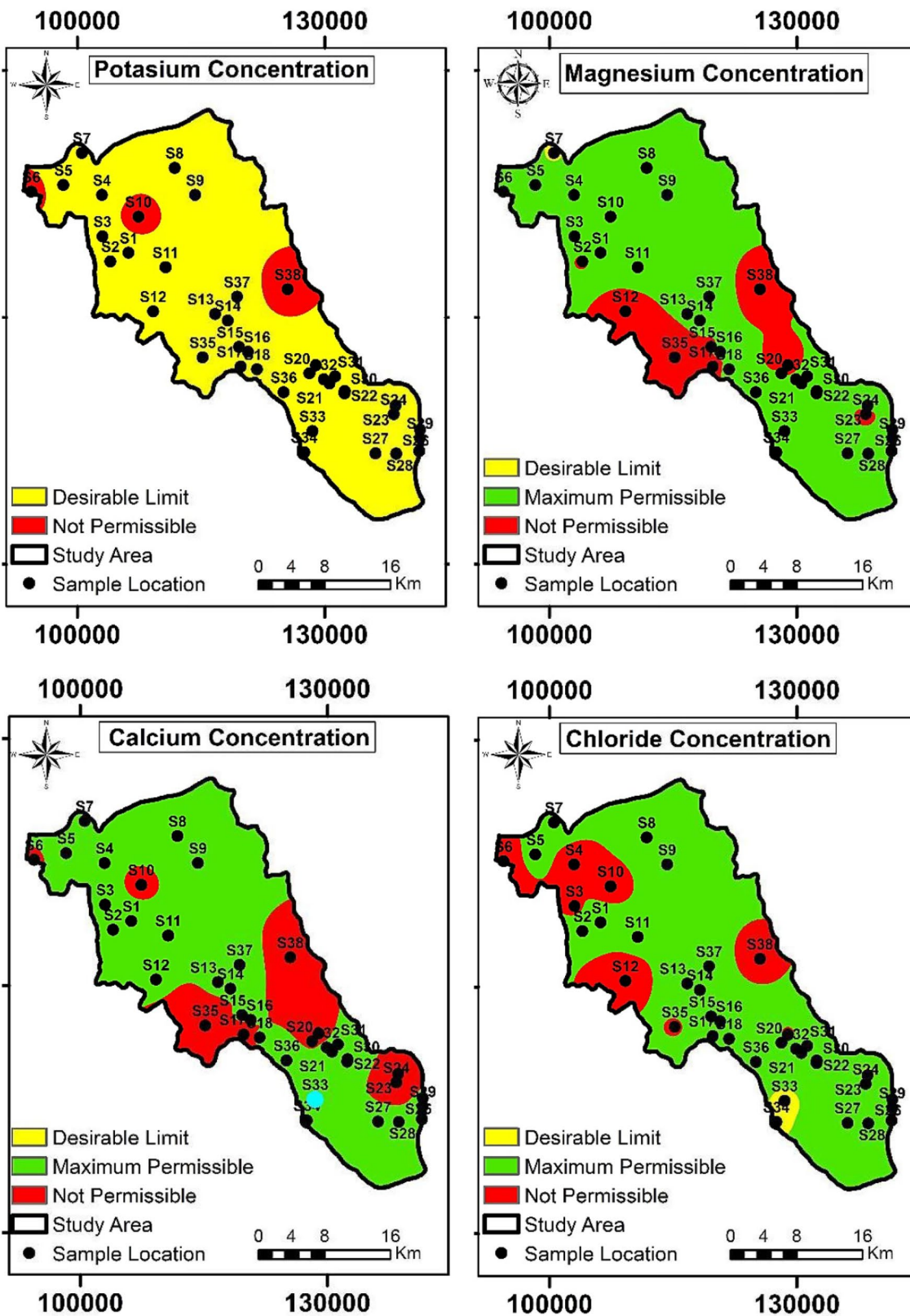**Fig. 7** Spatial distribution of electrical conductivity, TDS, and pH in the study area

Fig. 8 Spatial distribution of potassium, magnesium, calcium, chloride, sodium, nitrate, and sulphate in the study area
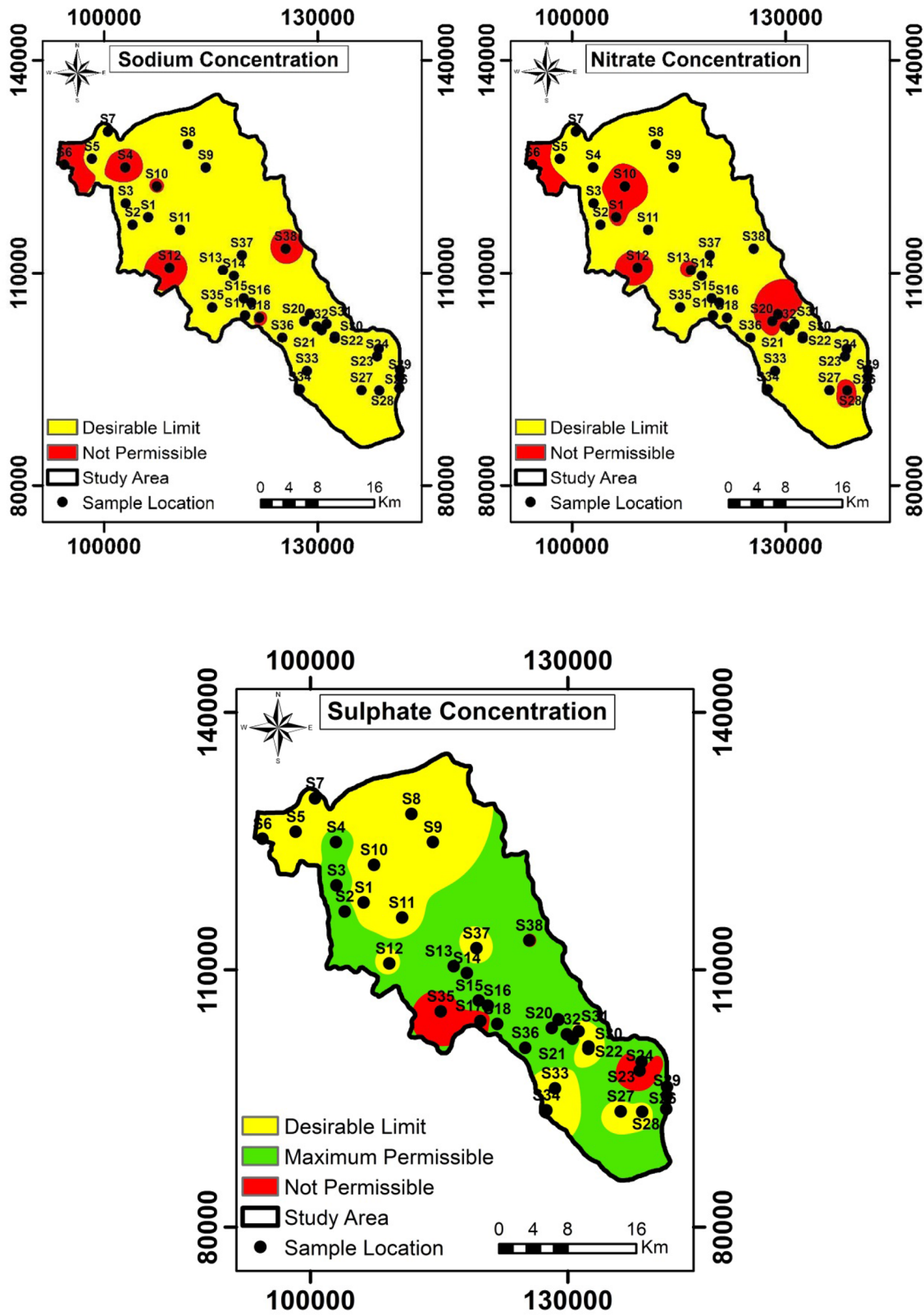
Fig. 8 (continued)

Table 3 Weight and relative weight of each parameter used for the WQI calculation

Physicochemical parameters	WHO Standard (2011)	Weight (w_i)	Relative weight (W_i)
pH	6.5–8.5	4	0.114
EC (μs/cm)	500	4	0.114
TDS (mg/l)	500	5	0.142
Cl (mg/l)	250	3	0.086
SO$_4$ (mg/l)	250	4	0.114
NO$_3$ (mg/l)	45	5	0.142
HCO$_3$ (mg/l)	120	3	0.086
Na (mg/l)	200	2	0.057
Ca (mg/l)	75	2	0.057
Mg (mg/l)	50	1	0.029
K (mg/l)	12	2	0.057
		35	0.998

$$w_i = w_i \bigg/ \sum_{i=1}^{n} w_i \qquad (2)$$

where W_i is the relative weight, w_i is the weight of each parameter physiochemical, and n is the number of parameters.

In the 3 step, the quality rating scale (q_i) for any parameter was determined using Eq. (3).

$$q_i = (c_i/s_i) \times 100 \qquad (3)$$

where q_i is the quality rating, C_i is the concentration of each chemical parameter in each water sample, and S_i is the drinking water standard for each chemical parameter according to the guidelines of the WHO [33].

In the final step, the S_{ii} is first determined for each chemical parameter Eq. (4), which was then used to calculate the WQI as per the following Eq. (5):

$$s_{ii} = w_i \times q_i \qquad (4)$$

$$WQI = \sum SI_i \qquad (5)$$

where S_{ii} is the subindex of all variables; the value is between 0 and 100 and q_i is the rating based on concentration of the parameter Tables 1 and 3.

WQI range and category of water can be classified in Table 4; in this study, the calculated WQI values have a range from 82.3 to 390.9 and this can be categorized into 4 water types, good water to unsuitable water for drinking (Table 4). This indicates that no sample location comes under "excellent category".

The calculation of WQI for groundwater samples is shown in (Table 5). A total of 38 samples were analysed for

Table 4 Water Quality Classification based on WQI

WQI range	Type of water
< 50	Excellent water
50–100	Good water
100–200	Poor water
200–300	Very poor water
> 300	Unfit for drinking

Table 5 Water quality index (WQI) classification for individual samples

| Sample	WQI	Classification
S1	169.5	Poor water
S2	221.8	Very poor water
S3	214.1	Very poor water
S4	248.2	Very poor water
S5	171.8	Poor water
S6	315.2	Unfit for drinking
S7	132.3	Poor water
S8	183.5	Poor water
S9	174.9	Poor water
S10	251.0	Very poor water
S11	176.9	Poor water
S12	308.1	Unfit for drinking
S13	194.8	Poor water
S14	202.2	Very poor water
S15	192.6	Poor water
S16	179.9	Poor water
S17	281.9	Very poor water
S18	184.2	Poor water
S19	390.9	Unfit for drinking
S20	183.9	Poor water
S21	221.2	Very poor water
S22	107.5	Poor water
S23	118.9	Poor water
S24	341.7	Unfit for drinking
S25	168.7	Poor water
S26	151.7	Poor water
S27	121.0	Poor water
S28	141.6	Poor water
S29	145.3	Poor water
S30	114.5	Poor water
S31	109.5	Poor water
S32	147.5	Poor water
S33	86.9	Good water
S34	82.3	Good water
S35	337.7	Unfit for drinking
S36	129.0	Poor water
S37	128.0	Poor water
S38	366.8	Unfit for drinking
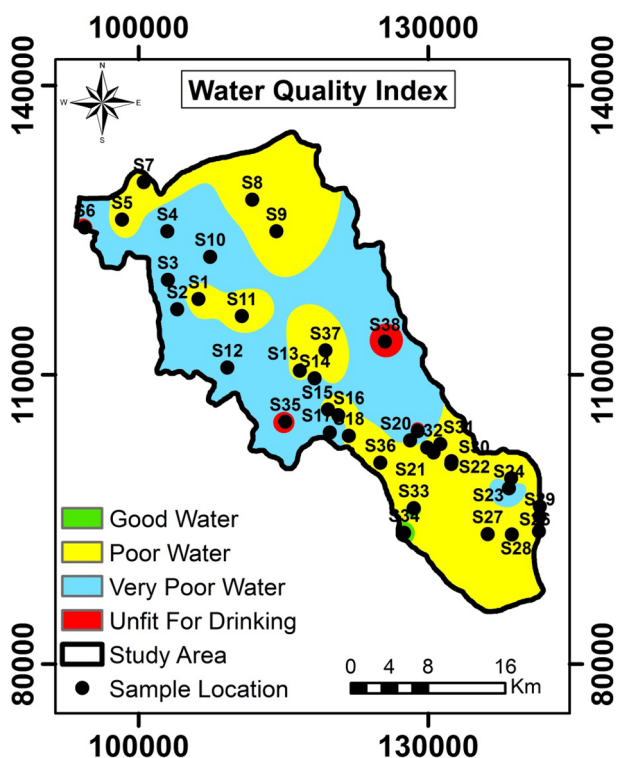
Fig. 9 Spatial distribution of groundwater quality index in the study area

WQI. The results show that 6% of the groundwater samples come under 'Good category', 61% of the samples belong to 'poor category', 18% come under 'Very Poor category', and 16% have been registered under the 'Unfit category'. The WQI shows that 5% of groundwater samples were found as good water.

The spatial distribution of WQI (Fig. 9) shows that groundwater with very poor quality is observed in the central and downstream part of the study area, while water with poor quality is recorded in the north and east. This deterioration of the quality of the subterranean waters could be explained by the dissolution of the evaporation formations rich in salts (halite, gypsum, and anhydrite), the contamination by livestock waste, the remoteness of the recharge zone of the aquifer studied, and by the residence time. From this classification, it can be concluded that the use of groundwater in the studied aquifer requires treatment before consumption.

6 Conclusions

In arid and semi-arid zones, groundwater is an essential element for socio-economic development. In recent decades, this resource has experienced significant qualitative

and quantitative degradation. For this reason, the krimat aquifer of the Essaouira basin was used as an example.

To evaluate the state of this resource, we used the hydrogeochemical approach based on the WQI index and a geographical information system.

The study of chemical facies shows that the groundwater of the study area is of type Ca–Mg–Cl and Ca–SO_4 with the dominance of the first type. Evaluation of physical parameters (pH and electrical conductivity (EC)) shows those groundwater is neutral with generally high mineralization. Indeed, 90% of the analysed samples have EC values higher than 1500 μs/cm reflecting a poor quality (no admissible). The spatial distribution of the chemical elements shows that the highest concentrations are observed in the central and downstream part of the study area, following the dissolution of the evaporite formations rich in salts and the remoteness of the recharge zone.

The results of the calculation of WQI show that 6% of the samples are classified as "Good", 61% in the "poor" category, 18% in the "Very poor" category, and 16% in the "unsuitable for drinking" class.

The spatial distribution of groundwater quality shows that groundwater with very poor quality is observed in the central and downstream part of the study area, while poor quality water is recorded in the north and east. This could be explained by the dissolution of the evaporation formations rich in salts (halite, gypsum, and anhydrite), the contamination by livestock waste, the remoteness of the recharge zone of the aquifer studied, and time of residence. This classification makes it possible to conclude that the use of groundwater in the studied aquifer requires pre-treatment for consumption.

However, the results obtained could be a basis for regional decision-makers for better management, planning, and protection of this resource.

Compliance with ethical standards

References

1. He J, Ma J, Zhao W, Sun S (2015) Groundwater evolution and recharge determination of the Quaternary aquifer in the Shule River basin, Northwest China. Hydrogeol J 23:1745–1759
2. Bahir M, Ouhamdouch S, Carreira PM, Zouari K (2019) Relationship between hydrochemical variation and the seawater intrusion within coastal alluvial aquifer of Essaouira basin (Morocco) using HFE-diagram. Springer, Cham
3. Azhar S, Ahmad ZA, Mohd KY, Mohammad FR, Hafizan J (2015) Classification of river water quality using multivariate analysis.

Procedia Environ Sci 30(1):79–84. https://doi.org/10.1016/j.proenv.2015.10.014

4. Hamed Y, Hadji R, Redhaounia B, Zighmi K, Bâali F, El Gayar A (2018) Climate impact on surface and groundwater in North Africa: a global synthesis of findings and recommendations. Euro-Mediterr J Environ Integr 3:25. https://doi.org/10.1007/s41207-018-0067-8

5. Aly A (2015) Hydrochemical characteristics of Egypt western desert oases groundwater. Arab J Geosci 8:7551–7564

6. Sappa G, Ergul S, Ferranti F, Sweya LN, Luciani G (2015) Effects of seasonal change and seawater intrusion on water quality for drinking and irrigation purposes, in coastal aquifers of Dares Salaam, Tanzania. J Afr Earth Sci 105:64–84

7. Emenike CP, Tenebe IT, Omole DO, Ngene BU, Oniemayin BI, Maxwell O, Onoka BI (2017) Accessing safe drinking water in sub-Saharan Africa: issues and challenges in south-west Nigeria. Sustain Cities Soc 30:263–272. https://doi.org/10.1016/j.scs.2017.01.005

8. Besser H, Hamed Y (2019) Causes and risk evaluation of oil and brine contamination in the Lower Cretaceous Continental Intercalaire aquifer in the Kebili region of southern Tunisia using chemical fingerprinting techniques. Environ Pollut 253:412. https://doi.org/10.1016/j.envpol.2019.07.020

9. Bahir M, Ouhamdouch S, Carreira PM, Chkir N, Zouari K (2016) Geochemical and isotopic investigation of the aquifer system under semi-arid climate: case of Essaouira basin (Southwestern Morocco). Carbonates Evaporites 33(1):65–77

10. Bahir M, Carreira PM, Ouhamdouch S, Chamchati H (2017) Recharge conceptual model and mineralization of groundwater in a semiarid region; Essaouira basin (Morocco). Procedia Earth Planet Sci 17:69–72

11. Jalali M (2007) Salinization of groundwater in arid and semi-arid zones: an example from Tajarak, western Iran. Environ Geol 52:1133–1149

12. Carreira PM, Marques JM, Nunes D (2014) Source of groundwater salinity in coastline aquifers based on environmental isotopes (Portugal): natural vs. human interference. A review and reinterpretation. Appl Geochem 41:63–175

13. Ouhamdouch S, Bahir M, Souhel A, Carreira PM (2016) Vulnerability and impact of climate change processes on water resource in semi-arid areas: in Essaouira Basin (Morocco). In: Grammelis P (ed) Energy, transportation and global warming, green energy and technology. Springer, Basel, pp 719–736

14. Ouhamdouch S, Bahir M, Carreira PM (2017) Geochemical and isotopic tools to deciphering the origin of mineralization of the coastal aquifer of Essaouira basin, Morocco. Procedia Earth Planet Sci 17:73–76. https://doi.org/10.1016/J.PROEPS.2016.12.038

15. Horton RK (1965) An index number system for rating water quality. J Water Pollut Control Fed 37:300–305

16. Brown RM, McClelland NI, Deininger RA, Tozer RG (1970) Water quality index—do we dare. Water Sew Works 117(10):339–343

17. Todd DK (1980) Groundwater hydrology, 2nd edn. Wiley, New York, p 535

18. Singh PK, Tiwari AK, Panigarhy BP, Mahato MK (2013) Water qual- ity indices used for water resources vulnerability assessment using GIS technique: a review. Int J Earth Sci Eng 6(6–1):1594–1600

19. Tyagi S, Sharma B, Singh P, Dobhal R (2013) Water quality assessment in terms of water quality index. Am J Water Resour 1(3):34–38

20. Wang H, Jiang X-W, Wan L, Han G, Guo H (2015) Hydrogeochemical characterization of groundwater flow systems in the discharge area of a river basin. J Hydrol 527:433–441

21. Tiwari AK, Singh AK, Singh MP (2015) Hydrogeochemical analysis and evaluation of surface water quality of Pratapgarh district, Uttar Pradesh, India. Appl Water Sci 7(4):1609–1623. https://doi.org/10.1007/s13201-015-0313-z

22. Bahir M, Mennani A, Oliveira da Silva M, Blavoux B (2003) Impact de la sécheresse sur la ressource en eau en zone semi-aride: cas de l'aquifère barrémien-aptien de la zone côtière d'Essaouira (Maroc). Tecnología de la intrusión de agua de mar en acuíferos costeros: países mediterráneos, pp 785–796

23. Ouhamdouch S, Bahir M (2017) Climate change impact on future rainfall and temperature in semi-arid areas (Essaouira Basin, Morocco). Environ Process 4:975–990. https://doi.org/10.1007/s40710-017-0265-4

24. Lozes A (1959) Rapport de synthèse sur les études sismiques dans la zone côtière d'Essaouira, Rapport inédit, Office National de la Recherche Pétrole, Ref. 20048/25, Maroc

25. Jalal M (2001) Potentialitéshydrogéologiques du cénomano-turonien du basin synclinal de Meskala-Kourimat-Ida Ou Zemzem (Essaouira, Maroc). Thèse de doctorat, Université cadi Ayyad de Marrakech, p 192

26. Bahir M, Mennani A, Jalal M, Youbi N (2000) Contribution à l'étude des ressources hydriques du bassin synclinal d'Essaouira (Maroc). Estudios Geol 56:185–195

27. Hamed Y, Dassi L, Tarki M, Ahmadi R, Mehdi K, Ben Dhia H (2010) Groundwater origins and mixing pattern in the multilayer aquifer system of the Gafsa-South mining district: a chemical and isotopic approach. Environ Earth Sci. https://doi.org/10.1007/s12665-010-0806-x

28. Hamed Y, Ahmadi R, Demdoum A, BouriS Gargouri I, Ben Dhia H, Al-Gamal S, Laouar R, Choura A (2014) Use of geochemical, isotopic, and age tracer data to develop models of groundwater flow: a case study of Gafsa mining basin-southern Tunisia. J Afr Earth Sci 100:418–436

29. Mokadem N, Demdoum A, Hamed Y, Bouri S, Hadji R, Boyce A, Laouar R, Saad A (2016) Hydrogeochemical and stable isotope data of groundwater of a multi-aquifer system: northern Gafsa basin (Central Tunisia). J Afr Earth Sci 114:174–191

30. Besser H, Mokadem N, Redhaounia B, Ayadi Y, Faten K, Harabi S, Hamed Y (2018) Groundwater mixing and geochemical assessment of low enthalpy resources in the geothermal field of Southestern Tunisia. Eur Mediter J Environ Integr. https://doi.org/10.1007/s41207-018-0055-z

31. Kouassi AM, Mamadou A, Ahoussi KE, Biemi J (2013) Simulation de la conductivité électrique des eaux souterraines en relation avec leurs propriétés géologiques : cas de la Côte d'Ivoire. Rev Ivoir Sci Technol 21–22:138–166

32. Bouteraa O, Mebarki A, Bouaicha F, Nouaceur Z, Laignel B (2019) Groundwater quality assessment using multivariate analysis, geostatistical modeling, and water quality index (WQI): a case of study in the Boumerzoug-El Khroub valley of Northeast Algeria. Acta Geochim 38:796. https://doi.org/10.1007/s11631-019-00329-x

33. WHO (2011) WHO guidelines for drinking-water quality, 4th edn. World Health Organization, Geneva

34. ESRI (1999) ARCVIEW GIS v.10.2.2, Environmental Systems Research, Institute Inc

35. Hadji R, Yacine A, Hamed Y (2018) Using GIS and RS for slope movement susceptibility mapping: Comparing AHP, LI and LR methods for the Oued Mellah Basin, NE Algeria. In: Recent advances in environmental science from the Euro- Mediterranean and surrounding regions. doi: 10.1007/978-3-319-70548-4-536

36. Mokadem N, Redhaounia B, Besser H, Ayadi Y, Khelifi F, Hamad A, Hamed Y, Bouriet S (2018) Impact of climate change on groundwater and the extinction of ancient "Foggara" and springs systems in arid lands in North Africa: a case study in Gafsa basin (Central of Tunisia). Euro-Mediterr J Environ Integr 3:28. https://doi.org/10.1007/s41207-018-0070-0

37. Bouaicha F, Dib H, Bouteraa O, Manchar N, Boufaa K, Chabour N, Demdoumet A (2019) A Geochemical assessment, mixing behavior and environmental impact of thermal waters in the Guelma geothermal system. Algeria Acta Geochim 38:683. https://doi.org/10.1007/s11631-019-00324-2

38. Bouaicha F, Dib H, Belkhiri L, Bouaicha F, Manchar N, Chabour N (2017) Hydrogeochemistry and geothermometry of thermal springs from the Guelma region Algeria. J Geol Soc India 90:226. https://doi.org/10.1007/s12594-017-0703-y

39. Piper AM (1944) A graphical interpretation of water—analysis. Trans Am Geophys Union 25:914–928

40. Piper AM (1953) A graphical procedure in the geochemical interpretation of water analysis. Trans Am Geophys Union 2(5):914–928

41. Hamad A, Baali F, Hadji R, Zerrouki H, Besser H, Mokadem N, Legrioui R, Hamed Y (2018) Hydrogeochemical characterization of water mineralization in Tebessa-Kasserine karst system (Tuniso-Algerian Transboundry basin). Eur-Mediterr J Environ Integr 3:7. https://doi.org/10.1007/s41207-017-0045-6

42. Qin R, Wua Y, Xu Z, Xie D, Zhang C (2013) Assessing the impact of natural and anthropogenic activities on groundwater quality in coastal alluvial aquifers of the lower Liaohe River Plain, NE China. Appl Geochem 31:142–158

43. Ouhamdouch S, Bahir M, Ait-Tahar M, Goumih A, Rouissa A (2018) Physico-chemical quality and origin of groundwater of an aquifer under semi-arid climate. Case of the Barremo-Aptian aquifer of Essaouira basin (Morocco Occidental). J Mater Environ Sci 9:1022–1034

44. Sahu P, Sikdar PK (2008) Hydrochemical framework of the aquifer in and around East Kolkata wetlands, West Bengal, India. Environ Geol 55:823–835

45. Vasanthavigar M, Srinivasamoorthy K, Vijayaragavan K et al (2010) Application of water quality index for groundwater quality assess- ment: Thirumanimuttar sub-basin, Tamilnadu, India. Environ Monit Assess 171(1–4):595–609. https://doi.org/10.1007/s10661-009-1302-1

46. Tiwari AK, Singh PK, Mahato MK (2014) GIS-based evaluation of water quality index of groundwater resources in West Bokaro Coal field India. Curr World Environ 9(3):843–850. https://doi.org/10.12944/CWE.9.3.35

47. Wagh VM, Mukate SV, Panaskar DB, Muley AA, Sahu UL (2019) Study of groundwater hydrochemistry and drinking suitability through Water Quality Index (WQI) modelling in Kadava river basin India. SN Appl Sci 1:1251. https://doi.org/10.1007/s42452-019-1268-8